

Optical Frequency-Hop Multiple Access Communications System

Habib Fathallah, Leslie A. Rusch and Sophie LaRochelle
(fhabib@gel.ulaval.ca, rusch@gel.ulaval.ca and laroche@gel.ulaval.ca)
COPL, Department of Electrical and Computer Engineering
Laval University, Québec, Canada G1K 7P4
(418) 656-2906, (418) 656-3159 fax

Abstract - We propose fast optical frequency-hop code division multiple access (FH-CDMA) for high bandwidth local area networks. Encoding and decoding are achieved by tunable fiber Bragg gratings. Frequency hopping offers many advantages compared to the previously proposed optical CDMA multiple access techniques. The simultaneous utilization of the time and frequency domains offers notable flexibility in the selection of codes, however code families previously developed for radio frequency (RF) communications are not directly applicable to an optical FH-CDMA system. We propose codes to meet the special constraints imposed by our encoding device and present theoretical and simulation results for their performance.

Index Terms: Optical multiple access protocols; Direct Sequence CDMA; Frequency Encoded CDMA, and Frequency Hopping CDMA; Bragg grating.

1. Introduction

Code Division Multiple Access (CDMA) communications is a potential candidate for the upcoming generation of optical Local Area Networks (LAN). It can provide a flexible interconnection between a high number of active users in a high bit rate LAN. Other attractive implementation features of CDMA include relaxed requirements of wavelength control, and a decentralized and asynchronous access protocol. CDMA techniques fall into four broad categories: direct sequence (DS), frequency encoded (FE), time hopping (TH) and frequency hopping (FH). Optical CDMA systems have been proposed for the first three [1-3]. The agility of modern radio transmitters to quickly change transmission frequencies for FH-CDMA has no obvious corollary in optics. In [4], we recently proposed a novel optical frequency-hop encoder/decoder employing a strain-tuned multiple fiber Bragg grating. Frequency hopping CDMA allows the simultaneous and efficient utilization of the time and frequency domains and does not require chip synchronization. The architecture of the encoder/decoder pair is an important feature of every CDMA system, the functionality of which should provide for an efficient encoding and correlation of the code sequences. We demonstrate that the proposed device can successfully perform the encoding/decoding operations, achieving nearly ideal cross-correlation (or cross-talk) between different users' codes.

Multiple Bragg gratings are used to generate the CDMA hopping frequencies. Due to the linear "first in line, first reflected" nature of multiple Bragg gratings (see Figures 1 and 2), the time frequency hopping pattern is determined by the order of the grating frequencies in the fiber. By use of piezo-electric devices, the order of the center frequencies of the Bragg gratings

can be changed, effectively changing the hop pattern and therefore allowing for programmable codes (Figure 1).

In this paper we analyze the achievable performance in terms of system capacity and probability of error. The simultaneous utilization of the time and frequency domains in FH-CDMA offers notable flexibility in the selection of codes, more easily satisfying the required quasi-orthogonality (or transparency) between the simultaneous users than previously proposed non-coherent DS-CDMA. It is important to note that codes families previously developed for radio frequency (RF) communications are not directly applicable to an optical FH-CDMA system. Our encoding device imposes special constraints on code design.

In [3], Ziemann and Iversen proposed acoustically tunable optical filters (ATOF) to implement frequency encoded CDMA system. ATOFs can also be used for FH-CDMA to improve performance over FE-CDMA. However, the ATOF, as well as other available spectral slicing integrated devices, suffer from insertion losses. In this regard, multiple fiber gratings appear to be a very interesting solution.

In section 2, we introduce the FH-CDMA system model. We describe the proposed optical frequency hopping system in section 3 and develop a suitable sub-optimal family of codes. In section 4, we analyze the performance of the proposed system in terms of probability of error via analysis and simulation. We also compare the performance of FH system with some previously proposed non-coherent DS systems.

2. Frequency-Hop CDMA system

2.1 CDMA system model

We consider a typical fiber optic CDMA communications network with transmitter and receiver pairs, *i.e.*, K users share the same optical medium usually, but not exclusively, in a star architecture (Figure 1). Each information bit from user k is encoded onto a code sequence or "address"

$$c_k(t) = \sum_{j=1}^N d_{k,j} p_j(t - jT_c) \quad (1)$$

where N is the length of the code, $d_{k,j} \in \{0, 1\}$, for $1 \leq j \leq N$, is the j^{th} chip value of the k^{th} user's code and T_c is the chip duration. Let $c_k = [d_{k,1}, d_{k,2}, \dots, d_{k,N}]$ be the discrete form of the code. The chip signaling waveform $p_j(t)$, for $1 \leq j \leq N$, is usually assumed to be rectangular with unit energy. In our system $p(t)$ is the impulse response of a single grating. In our FH system, the chip pulses are generated in different and disjoint frequency sub-bands (pulses with different colors) (Figure 3). Each transmitter

broadcasts its encoded signal to all the receivers in the network. At reception, the received signal is a sum of all the active users' transmitted signals.

$$r(t) = \sum_{k=1}^K b_k \mathbf{c}_k(t - \tau_k) \quad (2)$$

where $b_k \in \{0,1\}$ and $0 \leq \tau_k \leq T_c$ for $k=1, \dots, K$, are the k^{th} user's information bit and time delay respectively. The receiver applies a matched filter to the incoming signal to extract the desired user's bit stream. For notational simplicity, we assume that the desired user's signal is denoted by $k=1$ and $\tau_1=0$. The matched filter output for bit duration T is thus

$$\begin{aligned} y &= \int_0^T \mathbf{c}_1(t) r(t) dt \\ &= b_1 \int_0^T (\mathbf{c}_1(t))^2 dt + \sum_{i=2}^K b_i \int_0^T \mathbf{c}_1(t) \mathbf{c}_i(t - \tau_i) dt \quad (3) \\ &= b_1 N + \text{MAI} \end{aligned}$$

where $T=NT_c$ is the duration of one data bit. The first term in (3) corresponds to the desired user, the second is multiple access interference (MAI). In most CDMA systems, the MAI is the most important noise source. For a large number of interfering users, the probability density function of the MAI is usually approximated to be Gaussian appealing to central limit theorem arguments. To reduce the effect of the MAI, orthogonal (or nearly orthogonal) codes are required. For non-coherent DS-CDMA, different families of codes called optical orthogonal codes (OOCs) have been developed with acceptable levels of cross-talk between users [8].

2.2 FH-CDMA and coding

In FH-CDMA, the l^{th} chip pulse is modulated with frequency offset f_l about the carrier frequency f_c ,

$$f_l = \mathbf{h}(l) \frac{B}{q} \quad l = 1, \dots, N, \text{ and } 1 \leq \mathbf{h}(l) \leq q \quad (4)$$

where B is the signal bandwidth, $\mathbf{h}(l)$ is the placement operator (also called the frequency hop pattern), and q is the number of available frequencies. The placement operator is a sequence of N ordered integers determining the placement of frequencies in the N available time slots. Each user selects a set of N frequencies from a set of q available frequencies $\mathbf{S} = \{f_1, f_2, \dots, f_q\}$,

where $N \leq q$. A convenient way of representing a frequency hop pattern is through a $N \times q$ matrix representing the time and frequency axis (Figure 3).

As mentioned in the introduction, most codes developed for radio FH-CDMA assume $N=q$. Only a few code families can be generalized for our case $N < q$; all are sub-optimal. In our system the number N corresponds to the number of gratings written in the detector. The number of available frequencies q is dictated by the limit of tunability of the gratings discussed further in section 3.1. In [9], Bin recently proposed a construction

algorithm of a new family of codes with $(N \leq q)$. This family falls into the category of so-called one-coincidence sequences and is characterized by the following three properties: 1) all of the sequences are of the same length (fixed by the number of gratings); 2) in each sequence, each frequency is used at most once; 3) the maximum number of hits between any pair of sequences for any time shift equals one. For interested readers, a survey paper on one-coincidence sequences was written by Shaar *et al.* [10]. In [4], we demonstrated the coding/decoding performance of our device using the so-called hyperbolic codes, a subclass of the one-coincidence sequence families.

Let $c_k(j)$ be the j^{th} chip of code \mathbf{c}_k . As in any CDMA system, the selected users' codes are chosen to satisfy the following three fundamental conditions. Firstly, the peak of the auto-correlation function

$$R_m(s) = \sum_{i=0}^N c_m(i) c_m(i-s) \quad -N+1 \leq s \leq N-1 \quad (5)$$

should be maximized for each code. Secondly, the side-lobes of this function should be minimized. Finally, the cross-correlation function

$$R_{m,p}(s) = \sum_{i=0}^N c_m(i) c_p(i-s) \quad -N+1 \leq s \leq N-1 \quad (6)$$

of each pair of sequences c_m and c_p should be minimized. These conditions constrain the physical positioning of the gratings on the fiber as well as their bandwidth. The relative distances between the gratings must be chosen to satisfy a given level of auto- and cross-correlation between the codes. This distance in turn determines the achievable bit rate.

2.3 Signal to interference ratio and Probability of error

The MAI in (3), modeled as the sum of $K-1$ independent random variables, has variance that can be approximated as

$$\sigma_{MAI}^2 = (K-1)\sigma^2 \quad (7)$$

where $\sigma^2 = \overline{\sigma_{m,p}^2}$ is the mean value of the variance of the cross-correlation between each pair of codes [7]

$$\sigma_{m,p}^2 = \frac{1}{2N-1} \sum_{s=-N+1}^{N-1} (R_{m,p}(s) - \bar{R}_{m,p})^2 \quad (8)$$

and $\bar{R}_{m,p}$ is the average value of the cross-correlation between codes m and p . The mean value of MAI can be similarly expressed as $\mu_{MAI} = (K-1)\bar{R}_{m,p}$. The signal to interference can then be easily derived

$$SIR = N^2 / (K-1)\sigma^2 \quad (9)$$

The output of the matched filter (3) is compared to the threshold $\eta = N/2 + \mu_{MAI}$ to decide if a bit was transmitted. Using the Gaussian assumption for the MAI, the probability of error for equiprobable data is given by

$$\begin{aligned}
P_e &= \text{Prob}(y \geq \eta | b_1 = 0) \cdot \text{Prob}(b_1 = 0) \\
&\quad + \text{Prob}(y \leq \eta | b_1 = 1) \cdot \text{Prob}(b_1 = 1) \\
&= \frac{1}{2} \left\{ \text{Prob}(y \geq \eta | b_1 = 0) + \text{Prob}(y \leq \eta | b_1 = 1) \right\} \quad (10) \\
&= Q \left(N / \sqrt{(K-1)\sigma^2} \right) = Q(\sqrt{SIR})
\end{aligned}$$

$$\text{where } Q(x) = \frac{1}{\sqrt{2\pi}} \int_x^{+\infty} e^{-\frac{u^2}{2}} du$$

In this paper, we analyze only the performance degradation due to the presence of multiple access interference. The effects of quantum noise and thermal noise are neglected. The interferometric beat noise effect between frequency slices is not addressed here. In the theoretic calculation of the variance of the multiple access interference (7) and (8) we assumed chip synchronization, while for simulation we considered the real asynchronous system. In a positive system the exact variance of MAI with arbitrary timing delays between users is less than its variance in a chip synchronous case. Salehi *et al.* [11] used this to demonstrate that synchronous DS-CDMA offers an upper bound on the exact probability of error

$$P_e(\text{exact}) \leq P_e(\text{chip synchronous case}) \quad (11)$$

This relationship holds for one-coincidence sequences, hence, is also true for optical FH-system.

3. System Description

3.1 The encoding device

The encoding device consists of a series Bragg gratings all written at the same wavelength λ_B [5]. Each grating can be tuned independently using piezo-electric devices to adjust the Bragg wavelength from λ_B to a given wavelength defined by the corresponding placement operator. One advantage of this approach is that only one phase mask is needed to write any encoder or decoder. The tuning of each device will determine the code used. The gratings will spectrally and temporally slice an incoming broadband pulse into several components as demonstrated by Chen *et al.* [6]. In the decoder, the peak wavelengths would be placed in reverse order of the encoder to achieve the decoding function, *i.e.*, matched filtering (Figure 1).

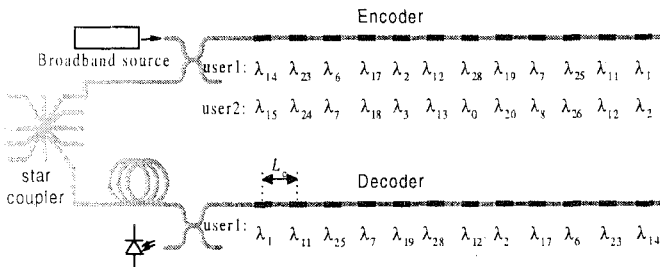


Figure 1: FH-CDMA communications system.

As illustrated in Figure 2, the reflected pulses are equally spaced at chip intervals T_c corresponding the round-trip propagation time between two gratings. Let L_c be the sum of one grating length and one spacing distance between adjacent grating pairs, c be the speed of light, n_{eff} be the average value of the effective refractive index; and n_g be the effective group index; then $T_c = 2n_g L_c / c$. The time spacing, the chip duration, and the number of gratings will limit the data bit rate of the system, *i.e.* all reflections should exit the fiber before the next bit enters. Each grating bandwidth is constrained so that the time overlap of the reflected pulses does not degrade the cross-correlation function. Therefore the total round trip time in a grating structure of N Bragg gratings is given by $2(N-1)L_c n_g / c$ effectively determining the bit duration T .

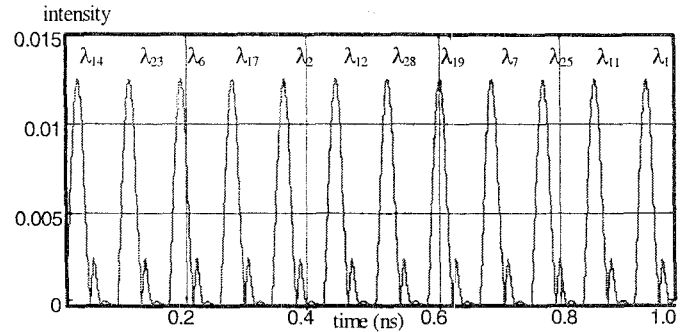


Figure 2: Reflected series of pulses from encoder 1 and their wavelengths.

In FH-CDMA, the frequency components are assumed to have a rectangular shape which require infinitely long Bragg gratings written with a sinc profile. In [4], we found that even for finite length profiles, the sinc main lobe apodization demonstrates high main lobe reflectivity (about 25 dB over the side lobes compared to 20 dB for the Gaussian profile).

3.2 Tunability of Gratings

For uniform gratings of a given reflectivity, the reflection bandwidth is inversely proportional to the grating length. For example, for wavelength λ the grating bandwidth between the two first zero crossings of the reflectivity spectrum is given by

$$\Delta\lambda_B = \frac{\lambda^2}{n_{eff} L} \sqrt{1 + (\kappa L / \pi)^2}$$

where κ is the coupling coefficient, L is the grating length. For a given fiber stretching ΔL , the shift in the peak Bragg wavelength $\Delta\lambda_s$ is function of the applied strain as expressed by $\Delta\lambda_s = 0.8\lambda(\Delta L / L)$ [11]. Therefore the number of available frequency bins is related to the fiber stretching by

$$q = \frac{\Delta\lambda_s}{m\Delta\lambda_B} = \frac{0.8\Delta L n_{eff}}{m\lambda \sqrt{1 + (\kappa L / \pi)^2}}$$

where m is a coefficient that takes into account the excess bandwidth left on each side of the main reflection lobe. For typical values of $\kappa L = 2$ (corresponding to 93% reflectivity), $n_{eff} = 1.452$, this requires that $\Delta L \approx m q \lambda_B$. Depending on the

available piezo-electric devices used for stretching, we can consider a tuning range of $0 \leq \Delta L \leq 50 \mu\text{m}$ which can lead to $0 \leq mq \leq 33$. Apodization usually leads to larger main lobe bandwidth and lower peak reflectivity, while it notably diminishes the side-lobe energy and hence the cross-talk. For our calculations we selected parameters leading to a nominal data rate of 1 Gb/s, fixing the total round trip time in the grating structure to $10^{-9} = 2(N-1)L_c n_{\text{eff}} / c$. Taking into account physical constraints in writing Bragg gratings (length L) and the spacing required between gratings to perform strain tunability, we selected $L=10$ mm with 8 mm spacing as reasonable values. This leads to $N=12$ for the number of gratings and a chip rate of $N \times 1 \text{ Gb/s} = 12 \text{ Gb/s}$. Figure 2 depicts a series of reflected pulses from an encoder of 12 gratings. Each pulse is on a different wavelength in the order specified by code 1.

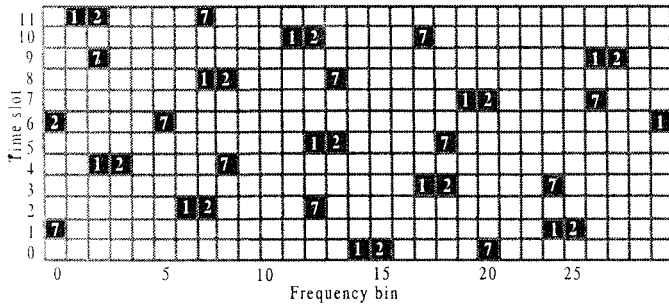


Figure 3: Three hopping patterns in a system with 12 time slots and 29 hop frequencies.

3.3 Code design for optical FH-CDMA

The previously developed codes in frequency hopping RF applications were mainly selected: 1) to reduce the Doppler effect; 2) to minimize the frequency synthesizer agility requirements; and 3) to reduce MAI in asynchronous systems. Also, most of them assumed that the number of available frequencies in the system is exactly equal to the number of chips (or hops) per bit. However, for our proposal only criterion 3 applies. Furthermore, the maximum number of hops is determined by the maximum number of gratings N that can be written in a fixed fiber length dictated in turn by 1) the required fixed bit rate; 2) each grating length, and 3) required physical spacing allowing tunability. The number of frequencies, however, is dictated by the tunability limitation of the gratings. These points lead to new relevant optimization criteria in frequency hopping code design.

L. Bin [9] recently proposed a novel FH-code generation algorithm. These codes fall into the category of one-coincidence sequences introduced in section 2, and guarantee minimum specified distances between adjacent symbols (or pulses). For our system, this means that the reflected frequency bins from adjacent pairs of gratings, (leading to two adjacent reflected pulses), are separated by a specified minimum number of bins. In our case, this reduces the effect of side lobes in the reflectivity of each grating. We describe the main steps of the algorithm in the appendix. Using $q=29$, and $N=12$, we derive 29 one-coincidence sequences, including $\mathbf{c}_1=[14 \ 23 \ 6 \ 17 \ 2 \ 12 \ 28 \ 19 \ 7 \ 25 \ 11 \ 1]$ and $\mathbf{c}_2=[15 \ 24 \ 7 \ 18 \ 3 \ 13 \ 0 \ 20 \ 8 \ 26 \ 12 \ 2]$. Figure 2 illustrates the

frequency-hop patterns of codes 1, 2 and 7. Reflected frequency bins from adjacent pairs of gratings are spaced at least by $d=8$ bins (see the appendix) which reduces the interference between the codes. Figure 4 a) and b) depict respectively the transmitted spectrum for user 1 and the delay time curves of each frequency bin, corresponding to the frequency-hop pattern of code 1.

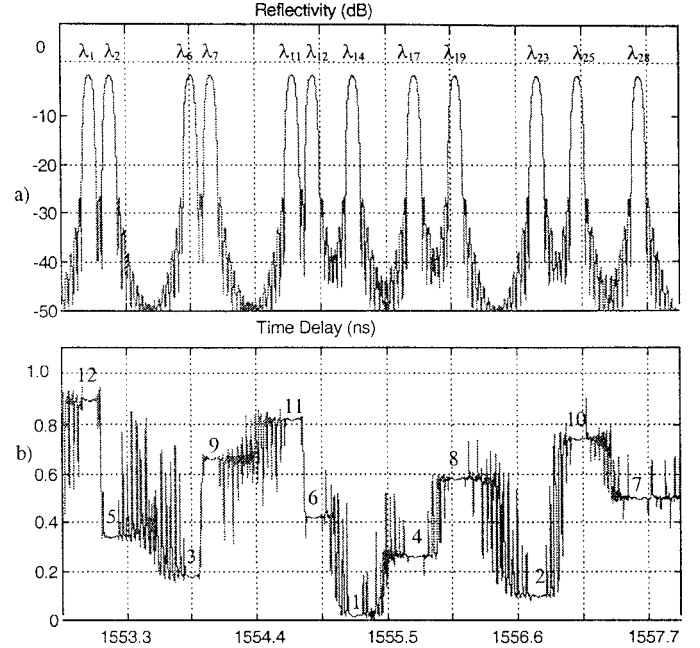


Figure 4: a) reflected spectrum from encoder 1, b) the group delay for each frequency bin.

4. Performance Analysis

4.1 Optical FH-CDMA vs. non-coherent DS-CDMA

We compare the capacity of both FH-CDMA and non-coherent DS-CDMA in terms of simultaneous number of users, *i.e.*, the number of codes with specified cross-correlation. Each family of optical orthogonal codes (OOC) for DS-CDMA are usually characterized by the quadruple $(n, w, \lambda_a, \lambda_c)$ where n denotes the sequence length, w is the sequence weight and λ_a and λ_c the maximum auto-and cross-correlation respectively [8]. As FH codes are two dimensional the effective length is $n=N \times q$. In Figure 5, we reproduce results from [8] which compare some DS-code families in terms of achievable probability of error as function of the simultaneous number of users. We compare them with our developed sub-optimal codes. FH-codes for $N=12$ and $q=19, 23, 27$ and 29 corresponding respectively to quadruples $(12 \times 19=228, 12, 0, 1)$, $(12 \times 23=276, 12, 0, 1)$, $(12 \times 27=324, 12, 0, 1)$, $(12 \times 29=348, 12, 0, 1)$, clearly outperform DS-codes of even greater length, including prime sequences (PS), quadratic congruence codes (QC), extended quadratic congruence codes (EQC) and truncated Costas array codes (TC).

4.2 Probability of error

Simulations were run for Bragg gratings of length 10 mm, spacing of 8 mm and a main lobe sinc apodization. The average variance for the simulated gratings was calculated per (8).

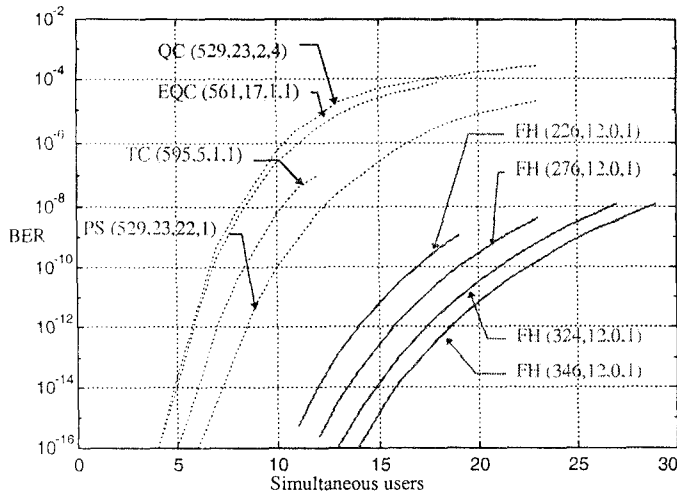


Figure 5: Probability of error vs. simultaneous number of users: FH and DS-CDMA.

For $N=12$, $q=29$, Figure 6 depicts the probability of error (10) versus the number of asynchronous simultaneous users; the interference contribution is assumed to have a Gaussian distribution. The upper bound (solid line) is derived assuming ideal reflectivity, and perfectly rectangular, disjoint, *contiguous* chip pulses. The simulated gratings (points) use non-ideal reflectivity, yet have better performance as we are able to take advantage of the spacing in time between chip pulses imposed by the linear array of Bragg gratings. Thus, simulation results confirm good performance, even for non-ideal reflectivity.

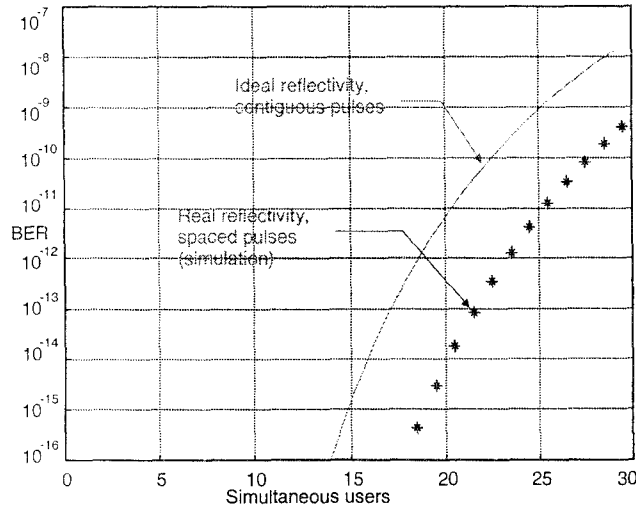


Figure 6: Probability of error vs. number of simultaneous users: simulation vs. ideal reflectivity.

5. Conclusion

We analyzed a novel high bandwidth optical frequency-hop CDMA communication system. Encoding/decoding operations are passively and efficiently performed using all optical, all fiber device. We proposed a sub-optimal family of codes. We emphasized the performance degradation due to multiple access interference. Optical FH-CDMA offers a large number of simultaneous users' codes with good transparency (low cross-talk) and, as demonstrated, optical FH-CDMA easily

outperforms non-coherent DS-CDMA.

References

1. J. Salehi, "Code Division Multiple-Access Techniques in Optical Fiber Networks- Part 1: Fundamental Principles" *IEEE Transactions on Communications*, vol. 37, no. 8, pp. 824-833, Aug. 1989.
2. D. Zaccarin, and M. Kevehad, "An Optical CDMA System Based on Spectral Encoding of LED" *IEEE Photonics Technology Letters*, vol. 4, no. 4, pp. 479-482 1993.
3. O. Zeiman and K. Iversen, "On Optical CDMA Based on Spectral Slicing Encoding with Integrated Optical Devices" *SPIE Proceedings*, vol. 2614, pp. 142-152, 1995.
4. H. Fathallah, S. LaRochelle, L.A. Rusch "Analysis of an optical frequency-hop encoder using strain-tuned Bragg gratings" submitted to *OSA Topical Meeting on Bragg Gratings, Photosensitivity, and Poling in Glass Fibers and Waveguides: Applications and Fundamentals*, Oct. 1997.
5. K. O. Hill, G. Meltz, "Fiber Bragg Grating Technology Fundamentals and Overview" *IEEE Journal of Lightwave Technology*, vol. 15, no. 8, pp. 1263-1276, 1997.
6. L. Chen, S. Benjamin, P. Smith, J. Sipe, "Ultrashort Pulse Reflection From Fibre Gratings: A Numerical Investigation" to be published *IEEE Journal of Lightwave Technology*, 1997.
7. Chung, J. Salehi, and V. Wei, "Optical Orthogonal Codes: Design, Analysis, and Applications" *IEEE Transactions on Information Theory*, vol. 35, no. 3, pp. 595-604, May 1989.
8. V. Maric, M. D. Hahm, and E. L. Titlebaum, "Construction and Performance Analysis of a New Family of optical Orthogonal Codes for CDMA Fiber-Optic Networks" *IEEE Transactions on Communications*, vol. 43, no. 2/3/4, pp. 485-489, 1995.
9. L. Bin, "One-Coincidence Sequences with Specified Distance Between Adjacent Symbols of Frequency-Hopping Multiple Access" *IEEE Transactions on Communications*, vol. 45, no. 4, pp. 408-410, April 1997.
10. Shaar, & P. Davies, "A survey of one coincidence sequences for frequency-hopped spread spectrum systems" *IEE Proceedings*, vol. 131, no. 7, pp. 719-724, April 1984.
11. Salehi, and C. A. Brackett, "Code Division Multiple-Access Techniques in Optical Fiber Networks- Part 2: Systems Performance Analysis" *IEEE Transactions on Communications*, vol. 37, no. 8, pp. 834-842, Aug 1989.
12. Ibsen, B.J. Eggleton, M. Sceats & F. Ouellette, "Broadly tunable DBR fibre laser using sampled fiber Bragg gratings" *Electronics Letters*, vol. 31, no. 1, pp. 37-38, Jan. 1995.

Appendix

Let q be an odd integer, and define $N = 2k = q - 2d - 1$. Let $\mathbf{C} = (c_0, c_1, \dots, c_{2k-1})$ be a permutation of $\mathbf{D} = (d+1, d+2, \dots, q-d-1)$. Let

$$D_n(j) = \left(\sum_{i=n}^{(n+j-1) \bmod [2k]} c_i \right) \bmod [q], \text{ for } 0 \leq n \leq 2k-1, \text{ and } 2 \leq j:$$

We select \mathbf{C} among the all the possible permutations of \mathbf{D} , which satisfies:

1. $c_i + c_{i+k} = q$, and $0 \leq i \leq k-1$
2. For each j , $2 \leq j \leq k$, all the $D_i(j)$ are different for $0 \leq i \leq 2k-1$.

If the vector \mathbf{C} exists, it is called the generator sequence, and a set of q sequences are generated by

$$F_j = (D_0(1) + j, D_0(2) + j, D_0(3) + j, \dots, D_0(2k) + j),$$

where $0 \leq j \leq q-1$, and "+" is modulo- q addition.